Prog. Theor. Phys. Vol. 68, No. 1, July 1982, Progress Letters

# Projectile Breakup Effect on $^6$Li Elastic Scattering from $^{28}$Si and $^{40}$Ca Studied by Microscopic Coupled-Channels Method

Yukinori SAKURAGI, Masanobu YAHIRO*) and Masayasu KAMIMURA
*Department of Physics, Kyushu University, Fukuoka 812*
(Received January 22, 1982)

The $^6$Li breakup is treated with the coupled-discretized-continuum-channels method. The ground and continuum states of $^6$Li are described by the microscopic $\alpha$-d cluster model. Forward-angle cross sections are well reproduced. The breakup effect is strongly repulsive so as to shallow by half the too deep double-folded potential.

In extensive applications of the double-folding model[1a] (DFM) to nucleus-nucleus scattering, $^6$Li scattering is known to be anomalously difficult to reproduce as far as use is made of the bare normalization factor of $N_R=1.0$ for the double-folded real potential between $^6$Li and target nuclei. Independently on targets and bomberding energies, the real part is required to be weakened by about half[1)~4)] ($N_R\approx 0.5\sim 0.6$) so as to fit the experimental data.

It has often been said that the strong renormalization may be attributed to the breakup effect of $^6$Li nucleus which has a small $\alpha$-d threshold energy of 1.47 MeV. In fact, Thompson and Nagarajan[5] found recently a large effect of the $^6$Li breakup on elastic scattering on the basis of the three-body model with the adiabatic treatment[6] of the $^6$Li breakup; the effect gives rise to a good fit to the data at forward angles. Their result suggests that the strong renormalization is largely due to the breakup of $^6$Li ions. However, magnitude of the renormalization factor in DFM was not discussed because they took $\alpha$-target and d-target optical potentials and an $\alpha$-d point-cluster wave function of $^6$Li instead of starting with a nucleon-nucleon force and a microscopic $^6$Li wave function. Validity of the adiabatic approximation should be examined, because the approximation often overestimates the breakup effect[6),7)] due to neglecting an energy transfer.

The purpose of the present paper is to make a microscopic coupled-channels (CC) calculation of $^6$Li scattering with $^6$Li-breakup channels taken explicitly into account in the framework of the coupled-discretized-continuum-channels (CDCC) method of Refs. 7) to 10), and to investigate the relation between the projectile breakup effect and the strong renormalization factor in DFM.

Since it is desirable to construct the bound- and continuum-state wave functions of $^6$Li as precisely as possible, we do it on the basis of the totally antisymmetrized $\alpha$-d cluster model. Let $\varphi^{(\alpha)}$ and $\varphi_{1^+}^{(d)}$ denote the internal wave functions of $\alpha$ and d clusters. The $1^+$ ground-state wave function of $^6$Li may be described by

$$\phi_{01^+M}(^6\mathrm{Li},\ \mathrm{g.s.})=\mathcal{A}[\varphi^{(\alpha)}[\varphi_{1^+}^{(d)}\otimes u_{l=0}^{(1^+)}]_{1^+M}] \qquad (1)$$

and the continuum-state wave function with the $\alpha$-d relative momentum $\hbar k$ ($\hbar^2k^2/2\mu=\varepsilon$, $\varepsilon$ being the $\alpha$-d c.m. energy) by

$$\phi_{lIM}(^6\mathrm{Li},\ k)=\mathcal{A}[\varphi^{(\alpha)}[\varphi_{1^+}^{(d)}\otimes u_l^{(I)}]_{IM}]. \qquad (2)$$

Here, $\mathcal{A}$ is the total antisymmetrization operator. $u_l^{(I)}$ is the $\alpha$-d relative wave function with the angular momentum $l$.

In order to take the continuum $^6$Li-breakup channels into account in practical CC calcu-

*) Present address: Division of General Education, Shimonoseki University of Fisheries, Yoshimi, Shimonoseki 759-65.

lations, we follow the framework of CDCC method.[7)~10)] Namely, after calculating the $\phi_{lIM}(^6\mathrm{Li}, k)$ for $0<k<k_{\max}$, we discretize the $k$-continuum into $N_b$ bins with an equal width $\Delta k$ and average the $\phi_{lIM}(^6\mathrm{Li}, k)$ in each momentum bin; let denote the averaged wave packets by $\{\bar{\phi}_{lIM}(^6\mathrm{Li}, i); i=1\sim N_b\}$. We then solve the relative motion between the $^6$Li and target nuclei within the usual CC framework where the $^6$Li internal wave functions are given by $\phi_{01^+M}(^6\mathrm{Li}, \text{g.s.})$ and $\{\bar{\phi}_{lIM}(^6\mathrm{Li}, i); i=1\sim N_b\}$. Validity of this type of CDCC method was extensively examined in Refs. 7) and 10).

As for the point-nucleon density of the target nucleus, we take that of $^{28}$Si and $^{40}$Ca adopted in Ref. 2).

The real part of the diagonal and channel-coupling form factors in the CDCC method are microscopically calculated with the use of a nucleon-nucleon potential of the M3Y type[1a)] and an additional delta-function potential which is regarded to approximate a part of the nucleon exchange effect; the potentials*) adopted are the same as those used in usual DFM studies. The imaginary part of the form factors are constructed by multiplying the real part ($N_R=1.0$) by a common constant $N_I$ as often done in DFM studies.

Now, let us discuss how to calculate the microscopic $^6$Li wave functions $\phi_{lIM}(^6\mathrm{Li})$ of Eqs. (1) and (2). The radial part of $\varphi^{(\alpha)}$ and $\varphi_1^{(d)}$ are assumed to be given respectively by the internal wave functions of the $(0s)^4$ and $(0s)^2$ harmonic-oscillator shell-model configurations with an oscillator constant $m\omega/\hbar = 0.5\ \mathrm{fm}^{-2}$. The $u_l^{(I)}$ is assumed here to satisfy the equation

$$\sqrt{1-K}\left(-\frac{\hbar^2}{2\mu}\nabla^2+V_{\mathrm{eff}} + a_{I,l}V_{\mathrm{eff}}^{(\mathrm{SO})}-\varepsilon\right)\sqrt{1-K}\,u_{lm}^{(I)}=0\,, \qquad (3)$$

*) The explicit form is given by Eqs. (11) and (16) in Ref. 1a). Another case of Eqs. (10) and (16) gives almost the same final results of Figs. 3 to 5.

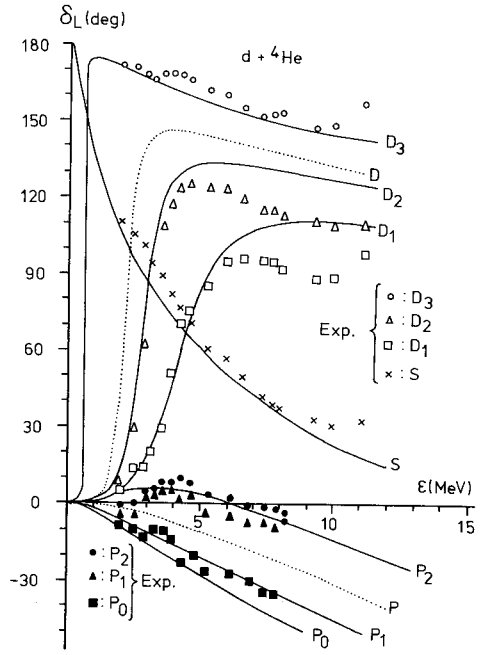


Fig. 1. $\alpha$-d scattering phase shifts for $l=0$, 1 and 2 waves. The solid lines are given by the microscopic $\alpha$-d cluster model. The dotted lines stand for the case of the $\alpha$-d spin-orbit potential switched off.

where $K$ is the exchange overlap kernel and $V_{\mathrm{eff}}(r)$*) and $a_{I,l}V_{\mathrm{eff}}^{(\mathrm{SO})}(r)$ are effective central and spin-orbit $\alpha$-d potentials, respectively, $a_{I,l}$ being $\{I(I+1)-l(l+1)-1(1+1)\}/2$. Equation (3) is a modified type[11)] of the equation of the orthogonality condition model[12)] and is considered to be a good approximation[13)] of the resonating group equation for $u_l^{(I)}$.

$V_{\mathrm{eff}}$ and $V_{\mathrm{eff}}^{(\mathrm{SO})}$ are so chosen as to fit well the low energy part ($\varepsilon\lesssim 15$ MeV) of the $\alpha$-d phase shifts (Fig. 1); also, the energies of the

*) The nuclear part is chosen at $V_{\mathrm{eff},l}^{(\mathrm{Nucl})}(r) = v_1\exp\{-(r/r_1)^2\}+v_2\exp\{-(r/r_2)^2\}$ with $v_1=-102.4$, $r_1=2.19$, $v_2=46.2$, $r_2=1.61$ for $l=0$, $v_1=-49.4$, $r_1=2.19$, $v_2=22.3$, $r_2=1.61$ for $l=1$ and $v_1=-83.0$, $r_1=2.38$, $v_2=31.0$, $r_2=1.85$ for $l=2$ ($v$'s in MeV and $r$'s in fm).

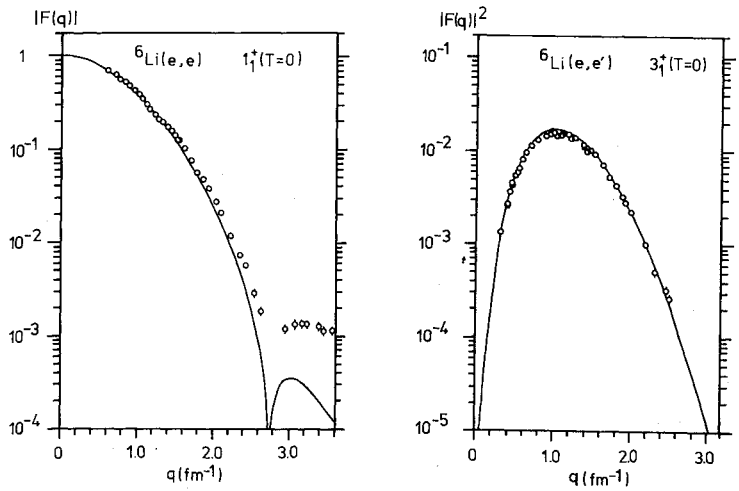


Fig. 2. Electron scattering charge form factors of $^6$Li. The solid lines are given by the microscopic $\alpha$-d cluster wave functions of the ground and 0.71 MeV $3^+$ states.

ground state and $3^+$ resonance at $\varepsilon=0.71$ MeV are fitted.

The microscopic wave functions of the ground state and the $3^+$ resonance are successfully examined by the elastic and inelastic electron scattering charge form factors (Fig. 2). The density of our $^6$Li ground state is very close to that adopted in Ref. 2).

As for those $\alpha$-d continuum states, we consider that, since the $^6$Li incident energies of 99 MeV and 156 MeV concerned in the present paper are rather high, the effect of the $\alpha$-d spin-orbit potential must play a minor role in calculating the $^6$Li elastic scattering angular distribution. We therefore switch off the $V_{\rm eff}^{(\rm so)}$ in Eq. (3) and reconstruct the $\alpha$-d wave functions (but note that the potential has been taken in the above examination).

Due to this approximation, the calculated $3^+$, $2^+$ and $1^+$ resonances in Fig. 1 become degenerate to a resonance at $\varepsilon\simeq 2$ MeV with the width of about 1 MeV. Taking this position and width into consideration, we discretize the $\alpha$-d continuum into two bins in each $\alpha$-d partial wave. We take $k_{\rm max}=1.0$ fm$^{-1}$ and therefore $\Delta k=0.5$ fm$^{-1}$. In the light of the CDCC analysis[7] of d+$^{58}$Ni scattering at $E_{\rm d}=80$ MeV, the present case $k_{\rm max}=1.0$ fm$^{-1}$ and $\Delta k=0.5$ fm$^{-1}$ is considered to be a good approximation of the exact calculation at forward angles in rather high-energy $^6$Li scattering. The $\alpha$-d relative waves of $l=0$, 1 and 2 are taken in the following calculation: We have verified that the effect of the $l=3$ and 4 waves is negligible for $^6$Li elastic scattering. Thus, the number of channels considered here amount to thirteen.

Figure 3 illustrates the angular distribution of elastic $^6$Li+$^{40}$Ca scattering at $E(^6\text{Li})=156$ MeV in ratio to the Rutherford cross section. The dashed line stands for the usual DFM calculation ($N_{\rm R}=0.64$ and $N_{\rm I}=0.68$) with the use of our $^6$Li ground-state density. The dotted line which lies far above the experimental data is a DFM result with $N_{\rm R}=1.0$ and $N_{\rm I}=0.68$. The solid line shows the present CDCC result with $N_{\rm R}=1.0$ and $N_{\rm I}=0.68$; it beautifully fits the data for $\theta_{\rm cm}\lesssim 25^\circ$. In order to see the breakup effect explicitly, we simply have taken the same imaginary potential as the DFM cases mentioned above and have not searched the best one which could improve the fit to the data at backward angles. Similar analysis is shown in Fig. 4

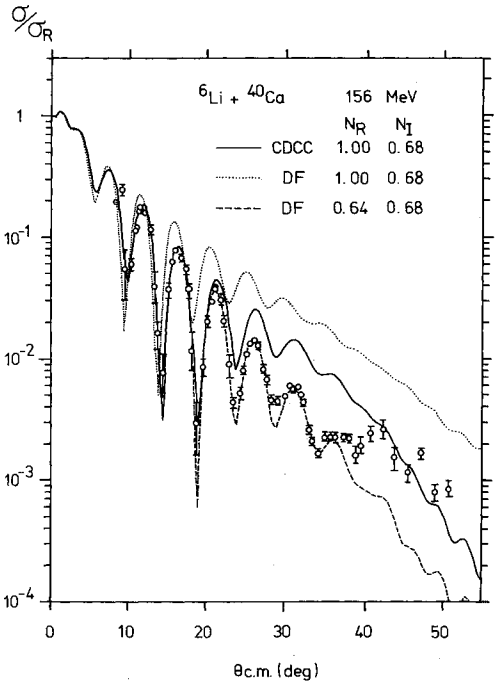


Fig. 3. Angular distribution of elastic $^6$Li scattering from $^{40}$Ca at $E(^6\text{Li})=156$ MeV. Calculated results by the present model (CDCC) and by the double-folding model (DF) are shown. The experimental data are from Ref. 14).

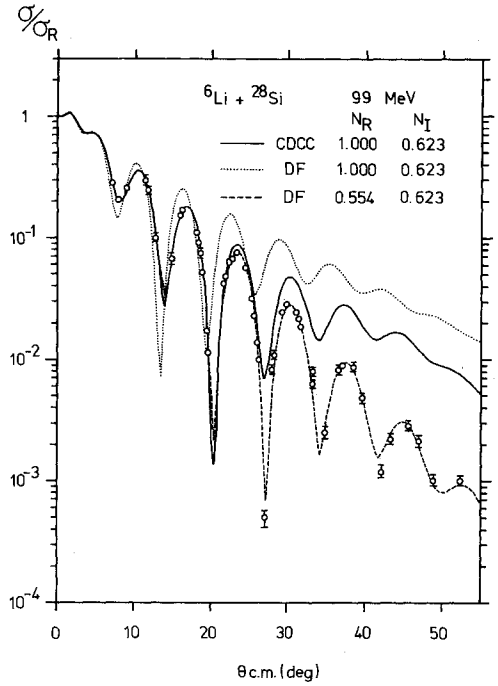


Fig. 4. Same as Fig. 3 for $^6$Li scattering from $^{28}$Si at $E(^6\text{Li})=99$ MeV. The data are from Refs. 2) and 15).

for $^6$Li+$^{28}$Si scattering at $E(^6\text{Li})=99$ MeV.

It can then be said that the strong renormalization of $N_R$ to about half (repulsive effect) in DFM comes from the $^6$Li breakup effect (as far as $\sigma(\theta_{cm})$ for $\theta_{cm}\lesssim 25^\circ$ is concerned). In order to clearly see the effectively repulsive role of the $^6$Li breakup, we plot in Fig. 5 the Argand diagram of the elastic S-matrix elements for the three cases of Fig. 3. We see that, for the scattering angular momentum $L\gtrsim 30$, the phases given by the CDCC calculation are shifted clockwise (effectively repulsive) relative to those given by DFM (namely, the $N_b=0$ case in the CDCC) with $N_R=1.0$ and $N_I=0.68$. In the surface region of the $^6$Li-target interaction, the breakup effect is repulsive since the grazing angular momentum is $L\simeq 35$. It is to be noted in Fig. 5 that the difference of the S-matrix elements themselves is so small between the CDCC result with $N_R=1.0$ and $N_I=0.68$ and the DFM result with $N_R=0.64$ and $N_I=0.68$.

As for the adiabatic approximation of the $^6$Li breakup, we have examined its validity with the use of the same three-body model of Ref. 5) and have found the approximation to be rather good at the energies considered here; the detailed discussion will be made in a forthcoming paper as well as discussion about roles of the individual $3^+$, $2^+$ and $1^+$ $\alpha$-d resonance states and the off-resonance continuum states. Application to $^7$Li scattering is in progress.

The authors would like to thank Professor M. Kawai and Mr. Y. Iseri for valuable discussions.

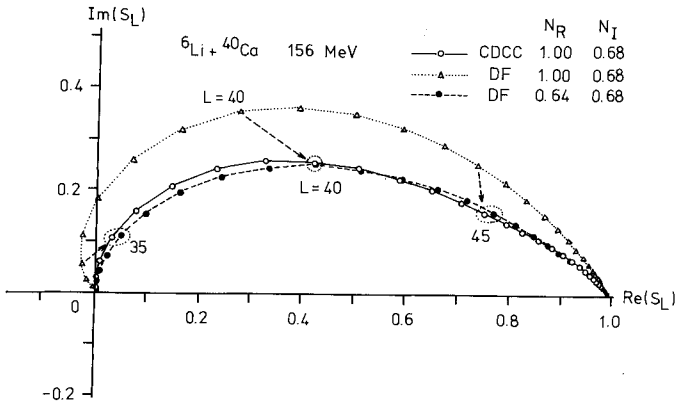


Fig. 5. Argand diagram of the elastic S-matrix elements for $^{6}$Li scattering from $^{40}$Ca.


1a) G. R. Satchler and W. G. Love, Phys. Reports **55** (1979), 183.
b) G. R. Satchler and W. G. Love, Phys. Letters **76B** (1978), 23.
2) D. P. Stanley, F. Petrovich and P. Schwandt, Phys. Rev. **C22** (1980), 1357.
3) J. Szymakowski, K. W. Kemper and A. D. Frawley, Nucl. Phys. **A355** (1981), 221.
4) C. B. Fulmer et al., Nucl. Phys. **A356** (1981), 235.
5) I. J. Thompson and M. A. Nagarajan, Phys. Letters **106B** (1981), 163.
6) H. Amakawa, A. Mori, H. Nishioka, K. Yazaki and S. Yamaji, Phys. Rev. **C23** (1981), 583.
7) M. Yahiro, M. Nakano, Y. Iseri and M. Kamimura, Prog. Theor. Phys. **67** (1982), 1467.
8) G. H. Rawitscher, Phys. Rev. **C9** (1974), 2210.
9) N. Austern, C. M. Vincent and J. P. Farrel, Jr., Ann. of Phys. **114** (1978), 93.
10) M. Yahiro and M. Kamimura, Prog. Theor. Phys. **65** (1981), 2046, 2051.
11) S. Saito, S. Okai, R. Tamagaki and M. Yasuno, Prog. Theor. Phys. **50** (1973), 1561. T. Matsuse and M. Kamimura, Prog. Theor. Phys. **49** (1973), 1765.
12) S. Saito, Prog. Theor. Phys. **41** (1969), 705.
13) A. Tohsaki-Suzuki, M. Kamimura and K. Ikeda, Prog. Theor. Phys. Suppl. No. 68 (1980), 359.
14) Z. Majka, H. J. Gils and H. Rebel, Z. Phys. **A288** (1978), 139.
15) P. Schwandt et al., Indiana University Cyclotron Facility Annual Report, 1979, p. 93 (unpublished).